Journal Pre-proofs

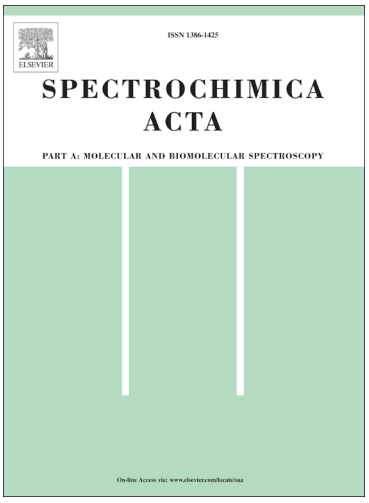

Novel insights on the Pd speciation in Pd/SSZ-13 and on the role of H_2O in the Pd reduction by CO

Sara Morandi, Lidia Castoldi, Roberto Matarrese, Luca Lietti

PII: S1386-1425(24)01111-9
DOI: https://doi.org/10.1016/j.saa.2024.124945
Reference: SAA 124945

To appear in: *Spectrochimica Acta Part A: Molecular and Biomolecular Spectroscopy*

Received Date: 13 February 2024
Revised Date: 11 July 2024
Accepted Date: 6 August 2024

Please cite this article as: S. Morandi, L. Castoldi, R. Matarrese, L. Lietti, Novel insights on the Pd speciation in Pd/SSZ-13 and on the role of H_2O in the Pd reduction by CO, *Spectrochimica Acta Part A: Molecular and Biomolecular Spectroscopy* (2024), doi: https://doi.org/10.1016/j.saa.2024.124945

Novel insights on the Pd speciation in Pd/SSZ-13 and on the role of H_2O in the Pd reduction by CO

Sara Morandi,*[a] Lidia Castoldi, [b] Roberto Matarrese [b] and Luca Lietti [b]

[a] *Department of Chemistry, NIS Center and INSTM Reference Center, Università di Torino, 10125 Torino, Italy*

[b] *Laboratory of Catalysis and Catalytic Processes, Department of Energy, Politecnico di Milano, Milano, 20156, Italy*

** Corresponding author: sara.morandi@unito.it*

Abstract

Pd speciation induced by the combined effect of CO and water on Pd/SSZ-13 samples prepared by both impregnation and ion exchange was examined by FT-IR spectroscopy of CO adsorbed at room temperature and at liquid nitrogen temperature on anhydrous and hydrated samples. Starting from the literature findings related to the CO reducing effect on Pd cations, the present work gives precise spectroscopic evidences on how water is necessary in this process not only for compensating with H^+ the zeolite exchange sites set free by Pd reduction, but also for mobilizing isolated Pd^{2+} / Pd^+ cations and making possible the reduction reactions. The aggregation of some Pd^+ sites, just formed by the reduction and mobilized by the hydration, gives rise to the formation of Pd_2O particles. Also, $Pd^0(100)$ sites are observed with CO on hydrated sample, formed by the aggregation and reduction of isolated Pd cations. Moreover, $Pd^0(111)$ sites are formed on the surface of PdO_x particles during CO outgassing. The observation of the combined effect of water and CO allowed to define assignments of IR bands related to carbonyls of Pd in different oxidation states and coordination degrees.

Keywords: Pd/SSZ-13, low-temperature NO_x adsorbers, PNA, water effect, CO adsorption, FT-IR spectroscopy.

1. Introduction

Pd-doped zeolites are widely employed as heterogeneous catalysts and adsorbers.[1-10] In these materials, exchanged metal ions inside the zeolite framework show interest as single atom materials. Among the big variety of zeolites, SSZ-13 is the most investigated due to the small pore sizes that suppress aggregation of metal cations under reaction conditions.

In the last years the interest towards Pd-exchanged zeolites increased due to their potential application as passive NO_x adsorbers (PNAs) to mitigate in vehicles the problem of cold-start NO_x emissions that significantly contribute to the atmospheric pollution.[11-13] These materials

are located upstream of the main catalytic converter and are designed to adsorb NO_x during the cold-start period, and to release the stored NO_x at higher temperatures when the downstream catalytic converter becomes efficient. In this application, Pd-containing zeolites emerged as the most promising materials thanks to their higher trapping efficiency, storage capacity and superior sulphur resistance if compared to other systems.[7,14-16]

Pd/zeolite materials prepared by both ion exchange and impregnation showed isolated Pd cations at the exchange sites inside the zeolite pores and PdO_x particles on the external surface.[17-20] Mandal et al. performed density functional theory (DFT) calculations and ab initio molecular dynamic (AIMD) simulations for constructing molecular models for isolated Pd cations charge-compensated by one or two tetrahedral aluminum sites in SSZ-13 zeolites.[21] By comparing the energies of different configurations, they demonstrated that, under dry conditions, Pd^+ and $[PdOH]^+$ species, exchanged at one Al site, prefer to locate in six-membered rings (6MR) and 8MR, respectively, while Pd^{2+} cations are more stable at the center of 6MR with the two aluminum sites on opposite positions of the ring. Symbolizing with Z the Si site substituted by Al, the above mentioned species can be denoted as ZPd^+, $Z[PdOH]^+$ and Z_2Pd^{2+}. Moreover, they demonstrated that, under dry conditions, Z_2Pd^{2+} is preferentially formed instead of ZPd^+ or $Z[PdOH]^+$ species, until saturation of two Al sites in 6MR. For a SSZ-13 with a Si/Al ratio of 9, the saturation of 2Al sites in 6MR theoretically occurs with a Pd/Al ratio of 0.146, i.e. about 1 wt.% of Pd.[22]

The nature of the Pd sites is affected by the presence of water. Mandal et al. studied the coordination of water molecules with exchanged Pd at 1Al and 2Al sites by computing the structures and the adsorption energies.[21] Under wet conditions, Z_2Pd^{2+} species can be converted into $Z[PdOH]^+$ and ZH^+ sites. However, the lowest energy species at low temperature and high water pressure is the completely hydrated $Z_2[Pd^{2+}(H_2O)_4]$ complex. An important finding is that the solvation operated by water molecules mobilizes isolated Pd^{2+} ions inside the zeolite channels.

In this frame, FT-IR spectroscopy is largely employed to determine the nature of Pd species and to derive mechanistic information about the Pd transformation. CO is a powerful probe molecule although the presence of a great variety of Pd carbonyl species makes the assignments of IR bands not always trivial and unambiguous. In particular, while there is a consensus to assign bands in the high-wavenumber region (2220-2180 cm^{-1}) to carbonyls of isolated Pd^{2+} ions at the zeolite exchange sites, i.e. Z_2Pd^{2+} species, band assignments in the spectral region 2180-2110 cm^{-1} are controversial.[17,18,23,24] In fact, in this region, bands with the same frequencies were assigned by some authors to carbonyls of Pd^+ and by other authors to carbonyls of $[PdOH]^+$ species. Moreover, many authors did not take into account the possibility that CO can be bonded on Pd cations belonging to PdO_x particles on the external surface of the zeolite. Besides, Kim et al.[25] showed, both through experiments and theoretical analysis, that Pd^{2+} can be reduced by CO involving H_2O molecules adsorbed on Brønsted acid sites of the zeolite according to the reaction:

$$CO + 2\ Z_2Pd^{2+} + ZH^+(H_2O) \rightarrow CO_2 + 2\ ZPd^+ + 3\ ZH^+ \qquad (1)$$

Water induces the reduction reaction in that it provides the protons to compensate the zeolite exchange sites.

On these bases, the present work is focused on the spectroscopic characterization of the Pd species present on Pd/SSZ-13 samples prepared by both impregnation and ion exchange techniques, aiming at the unambiguous identification of the Pd species. The characterization was performed by CO adsorption at room temperature (RT) and at liquid nitrogen temperature (T_{LN}) followed by FT-IR spectroscopy on anhydrous and hydrated samples. The rationalization of the combined effect of water, CO coverage and temperature on the nature of the CO adsorbed species allowed the unambiguous assignments of IR bands related to carbonyls of Pd in different oxidation states and coordination degrees, as will be reported in the following.

2. Experimental

The Pd-doped zeolites were prepared starting from a commercial SSZ-13 in the H-form (ACS Chemical, Si/Al = 10). The impregnated sample (Pd(i)/SSZ-13, nominal Pd loading 1 wt.%) was prepared by using an aqueous solution of $Pd(NO_3)_2$. The impregnating volume was 30% in excess with respect to the zeolite pore volume. More in detail, 1.1g of $Pd(NO_3)_2$ commercial solution (Pd 4.5% w/w, Alfa Aesar) were diluted in 100 ml of demineralized H_2O. Then, 5g of SSZ-13 powder were added under stirring; the resulting slurry was mixed at room temperature overnight and dried under vacuum at 80 °C.

The ion exchanged sample (Pd(ie)/SSZ-13) was obtained by adding 5 g of SSZ-13 powder to 5 mL of an aqueous solution of $Pd(NO_3)_2$ (0.19M). This concentration is higher than that used for the impregnation to consider the low efficiency of the ion exchange rection. The resulting slurry was stirred at 80 °C overnight, filtered and then dried under vacuum at 80 °C.

Both the dried precursors prepared by impregnation and ion exchange were calcined at 750 °C for 2h with a two-ramp heating program: from RT up to 500 °C (1 °C/min, hold at 500 °C for 3h) and then from 500 °C up to 750 °C (5 °C/min, hold at 750 °C for 2h).

Specific surface area, pore volume, crystalline structure and elemental analysis of the bare SSZ-13 and the as prepared Pd(i)/SSZ-13 sample were already reported in our previous paper and here summarized.[26] BET analysis performed by adsorption-desorption of nitrogen at -196 °C revealed values of specific surface area and pore volume of 558 m^2/g and 0.091 cm^3/g for the bare SSZ-13 and of 479 m^2/g and 0.063 cm^3/g for Pd(i)/SSZ-13. XRD patterns obtained for the parent SSZ-13 and Pd(i)/SSZ-13 are in agreement with the diffraction pattern of CHA zeolite framework: the addition of Pd neither modified the zeolite structure, nor led to the appearance of new phases. The elemental analysis performed by EDX and ICP-MS techniques confirmed a Si/Al ratio of 10 and a Pd loading of 1 wt.%. As for the ion exchanged sample, specific surface area and pore volume are 464 m^2/g and 0.059 cm^3/g. XRD pattern is in agreement with the diffraction pattern of CHA zeolite framework and the elemental analysis performed by EDX and ICP-MS techniques revealed a Pd loading of 0.2 wt.%.

Transmission Electron Microscopy (TEM) and High Resolution (HR)-TEM analyses were performed by using a side entry Jeol JEM 3010 (300 kV) microscope equipped with a LaB_6 filament. The samples were deposited on a copper grid coated with a porous carbon film; the digital micrographs were acquired by an Ultrascan 1000 camera and the images were processed by Gatan digital micrograph.

Absorption IR spectra were run on a Perkin-Elmer FT-IR 2000 spectrophotometer equipped with a Hg-Cd-Te cryodetector, working in the range of wavenumbers 7200-580 cm^{-1} at a resolution of 2 cm^{-1}. For the IR analysis, calcined powder samples were pelletized in self-

supporting disks (10-15 mg/cm^2) and placed in a quartz IR cell suitable for thermal treatments under controlled atmosphere. Spectra were recorded both at room temperature (RT) and at liquid nitrogen temperature (T_{LN}). Before IR measurements, the samples were outgassed at 500 °C for 30 min and then oxidized with 40 mbar of dry oxygen at 500 °C for 30 min. After oxidation, FT-IR spectra of CO under dry conditions were run at RT following two procedures: (i) at constant CO pressure (20 mbar) with spectra recorded at increasing contact time; (ii) at increasing CO pressure up to 20 mbar.

Concerning the measurements carried out under wet conditions, water (2 mbar) was added after the admission of 20 mbar of CO on the oxidized samples. Alternatively, before CO admission, the oxidized samples were contacted with H_2O (2 mbar) and then outgassed at RT. After this pre-hydration process carried out at RT, CO admission was performed at increasing pressure both at RT and at T_{LN}. In the Figures, if not differently stated, FT-IR spectra are always reported as difference where the subtrahend spectrum is that recorded after oxidation, i.e. before CO or H_2O admission. In the case of CO adsorbed on the pre-hydrated samples, the subtrahend spectrum is that recorded after oxidation and after water adsorption and outgassing at RT.

Since the results obtained in the case of the impregnated and ion exchanged samples are qualitatively very similar, in the following the IR spectra of Pd(i)/SSZ-13 sample will be mainly considered and discussed in detail. In fact, the main difference in terms of FT-IR spectra is related to the band intensities, much lower for the ion-exchanged sample with respect to the impregnated one due to the higher Pd content of this latter. For this reason, the results obtained over the Pd(i)/SSZ-13 will be mainly considered, and only few comparison data of the ion-exchanged sample will be shown.

3. Results and Discussion

Whatever the adopted synthesis method, i.e. ion exchange or impregnation, isolated Pd cations at the zeolite exchange sites and PdO_x particles on the external surface are formed, as well documented in the literature.[17-20] TEM and HR-TEM images of the freshly calcined Pd(i)/SSZ-13 and Pd(ie)/SSZ-13 samples shown in Figure 1 point out the presence of PdO_x particles with inhomogeneous sizes. The particles visible in the images show dimensions that are too big for the zeolite porosity, so that they are on the external surface. On the Pd(ie)/SSZ-13, PdO_x particles are less abundant than on Pd(i)/SSZ-13, as expected both from the different preparation methods and to the lower Pd loading (0.2 vs. 1 wt.%). For the impregnated sample, these images were already published in our previous papers.[20] Samples that underwent the outgassing and oxidation steps before the IR measurements showed the same features of the freshly calcined ones (not reported for sake of brevity).

At variance, the presence of isolated Pd ions formed by ion exchange with the Brønsted acid sites of the SSZ-13 has to be shown by CO adsorption followed by FT-IR spectroscopy. As already explained, since the spectroscopic results obtained for the impregnated and ion exchanged samples are very similar, in the following Pd(i)/SSZ-13 spectra are commented.

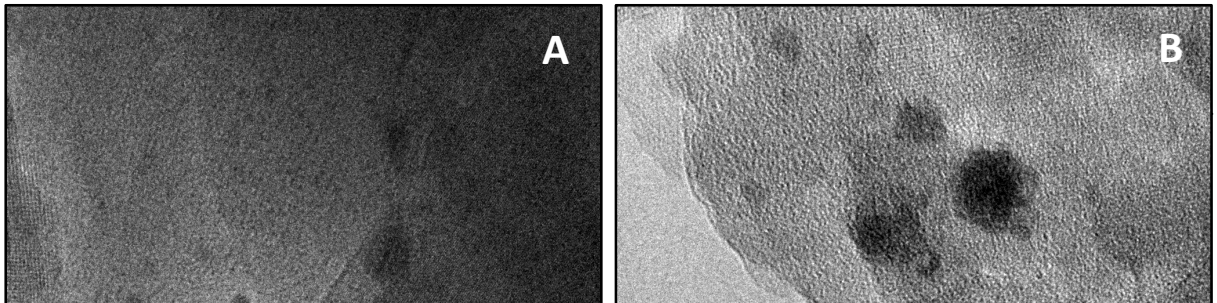

Fig. 1 TEM (panels A and C) and HR-TEM (panels B and D) images of the calcined Pd(i)/SSZ-13 sample (panels A and B, instrumental magnification: 120 and 300 kX, respectively) and Pd(ie)/SSZ-13 sample (panels C and D, instrumental magnification: 100 and 200 kX, respectively).

3.1. H_2O adsorption over Pd(i)/SSZ-13

The CO adsorption experiments have been performed over anhydrous/hydrated samples since the analysis of the water effect on the carbonyl species allowed their unambiguous band assignment; to this end water was admitted before and after CO.

Before describing the effect of water on the adsorbed carbonyl species, its adsorption alone has been considered; the FT-IR spectra obtained during the pre-hydration process are shown in Figure 2. The band at 1625 cm^{-1} is assigned to the OH bending mode of molecularly adsorbed water and the broad band present in the region 3600-2100 cm^{-1} is assigned to the stretching mode of H-bonded hydroxyls belonging to both molecularly adsorbed H_2O and OH groups formed by the dissociative chemisorption of water molecules. The Evans window in the region 2700-2500 cm^{-1}, due to a Fermi resonance and denoted by asterisk in Figure 2, evidences the adsorption of water molecules on the Brønsted acid sites of the zeolite through H-bond with the formation of complexes in which H_2O/ZH^+ ratio is 1:1.[27,28] Moreover, the sharp band at 3680 cm^{-1} denotes the formation of a not H-bonded hydroxyl family. This is a new OH family, not present on the sample after the oxidation treatment. Indeed, by the inspection of the spectrum reported in the inset of Figure 2, it is possible to observe that on the outgassed and oxidized sample, before water admission, three bands are present in the ν(O-H) spectral region. They are assigned to the stretching mode of the following species:[29] (i) isolated and terminal silanols (Si-OH), band at 3735 cm^{-1}; (ii) OH groups bonded to extra-framework aluminum, band at 3647 cm^{-1}; (iii) Brønsted acid sites, i.e. OH groups bridged on Si and Al, band at 3605 cm^{-1}. The absorption at 3680 cm^{-1} formed upon water admission is new and, on the base of DFT harmonic frequency computed by Mandal et al.,[21] it could be assigned to the O-H stretching mode of the $Z[PdOH]^+$ species.

Before CO adsorption, the sample was outgassed in order to remove excess water from the zeolite pores, since this may prevent CO to enter inside the zeolite framework.

After outgassing (Figure 2, trace b), a residual hydration is still present in form of both adsorbed molecular water (reasonably on both isolated Pd species and Brønsted acid sites of SSZ-13) and OH groups formed by dissociative chemisorption. The residual hydration, evaluated by TG/MS analysis, is about 10 wt.%.

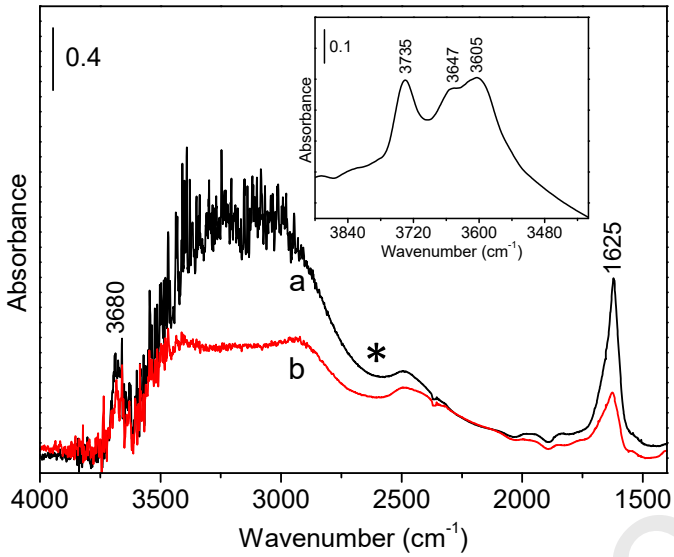

Fig. 2 FT-IR spectra obtained at RT after H_2O admission (2 mbar, trace a) and subsequent outgassing (trace b) on oxidized Pd(i)/SSZ-13. Evans window (*). Inset: spectral region of the ν(O-H) modes before water admission (this is not a difference spectrum).

3.2. CO adsorption over anhydrous Pd(i)/SSZ-13 and effect of hydration

Figure 3 compares FT-IR spectra obtained at constant CO pressure (20 mbar) and increasing contact time up to 1h on the anhydrous sample (panel A) and FT-IR spectra obtained at increasing contact time up to 1h after the subsequent addition of water (2 mbar) to the 20 mbar of CO (panel B). The spectra can be divided in two regions: the high-wavenumber region at the left of the green line in Figure 3 and the low-wavenumber one at the right. It is observed that under dry conditions (panel A) the high-wavenumber region shows carbonyl bands that prevail on carbonyl bands in the low-wavenumber one; the reverse is observed at the end of the hydration process reported in panel B. In particular, spectra in Figure 3B show, from blue to black trace, the erosion of the high-wavenumber bands and the increase of the low-wavenumber ones upon increasing H_2O contact time. The presence of an isosbestic point, evidenced by the green dotted line, clearly indicates the inter-conversion among different kind of carbonyl species. This inter-conversion in the presence of CO and H_2O puts in evidence an effect that CO cannot explicate under dry conditions. As reported by Kim et al.,[25] Pd^{2+} can be reduced by CO involving H_2O molecules adsorbed on Brønsted acid sites of the zeolite, following the reaction (1) previously reported. This means that the high-wavenumber bands are related to carbonyls of Pd^{2+} and the low-wavenumber ones are related to carbonyls of Pd^{+}. It is worth to note that, in literature, bands at wavenumbers lower than 2000 cm^{-1} are assigned to bridged carbonyls on Pd^0 particles (1960 cm^{-1}) and on Pd^{+} sites belonging to Pd_2O particles (1897 cm^{-1}).[30,31] Thus, it is possible to hypothesize a reduction process that leads up even to the formation of metallic Pd.

At variance, from the data showed in Figure 3, it cannot be excluded that bands in the low-wavenumber region might be related to hydrated species of Pd^{2+}, such as $Z[PdOH]^{+}$, as reported

by some authors.[18,23,24] For this reason, other CO adsorption experiments have been carried out and results are shown in the following.

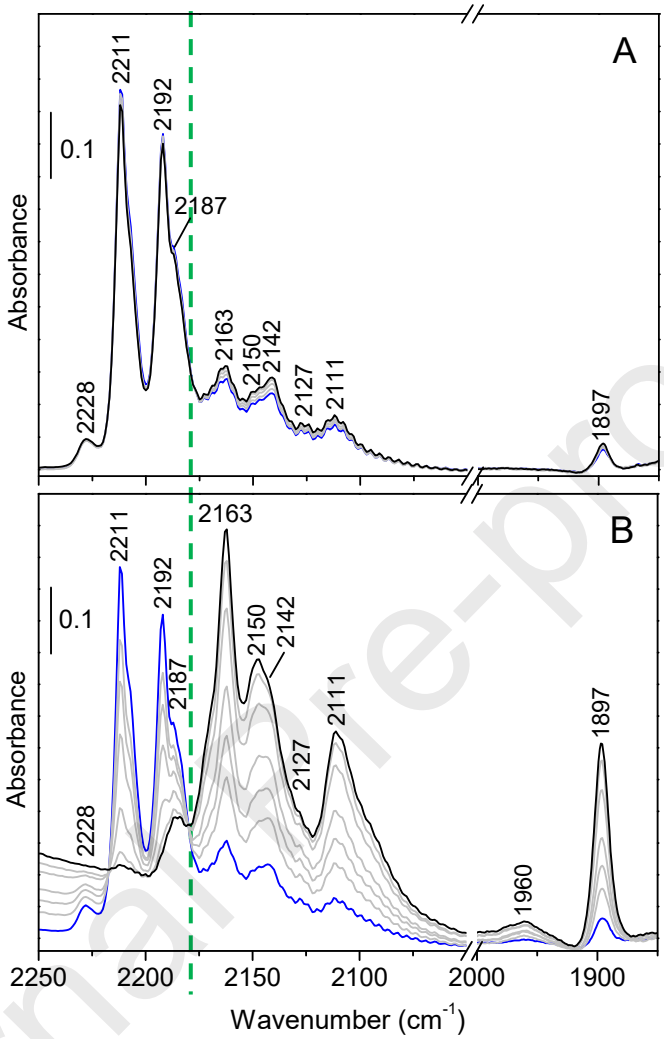

Fig. 3 FT-IR spectra of CO (20 mbar) adsorbed at RT on oxidized Pd(i)/SSZ-13. Panel A: spectra collected at increasing contact time up to 1h (from blue to black trace) under dry conditions. Panel B: blue trace is the spectrum of adsorbed CO (20 mbar) under dry conditions; the evolution from blue to black trace is obtained at increasing contact time up to 1h after H_2O addition (2 mbar). Green dotted line: separation between high- and low-wavenumber bands.

3.3. CO adsorption over pre-hydrated Pd(i)/SSZ-13

CO adsorption experiments have been carried out over the pre-hydrated sample and results are shown in Figure 4B. Water admission (2 mbar) at RT and subsequent outgassing at the same temperature leads to the spectrum already described in Figure 2; after hydration, CO adsorption was performed at increasing pressure up to 20 mbar. In Figure 4, CO spectra obtained for the pre-hydrated sample (panel B) are compared with the spectra obtained upon CO adsorption at increasing pressure on the anhydrous sample (panel A). Also in this case, the presence of the same two groups of bands is well evident, being the Pd carbonyl bands in the low-wavenumber region favorite by the presence of adsorbed water. It is possible to observe that on the pre-hydrated sample (Figure 4B) the high-wavenumber bands are not formed, except for that at 2187 cm^{-1}, and the low-wavenumber ones are immediately formed already at very low CO pressure. At variance, in the measurement shown in Figure 3B, one hour is necessary to completely transform the high-wavenumber bands into the low-wavenumber ones upon water addition. Based on these data, it is speculated that the kinetics observed when water was admitted after CO is not related to Pd reduction, but to the diffusion of water inside the zeolite pores and/or to hydration phenomena involving the Pd species.

In this respect, it is important to consider that the low-wavenumber bands formed upon hydration of the sample may be associated with hydrated species of Pd^{2+}, such as $Z[PdOH]^+$, and not to the reduction of Pd^{2+} to Pd^+ favored by water addition. To check this point, the reduction of Pd^{2+} by CO has been inhibited by operating at low temperature, and CO adsorption was carried out at liquid nitrogen temperature (T_{LN}). Also in this case, the sample was pre-hydrated by introducing water at RT and subsequently purged at RT. It was then cooled down using liquid nitrogen before introducing CO at increasing pressures. Figure 5 illustrates a comparison between the CO spectra obtained at T_{LN} after hydration at RT (panel B) and the CO spectra obtained at T_{LN} for the anhydrous sample (panel A). In both cases, the CO pressure was limited to 0.1 mbar. Indeed, unlike at RT, at T_{LN} higher pressures result in CO being adsorbed on the zeolite Brønsted acid sites and forming a liquid-like phase within the pores. These two phenomena are evidenced by the increase of two intense bands at approximately 2170 and 2140 cm^{-1}, respectively, when pressures exceed 0.1 mbar (spectra not shown). These bands overshadow the bands related to Pd carbonyls.

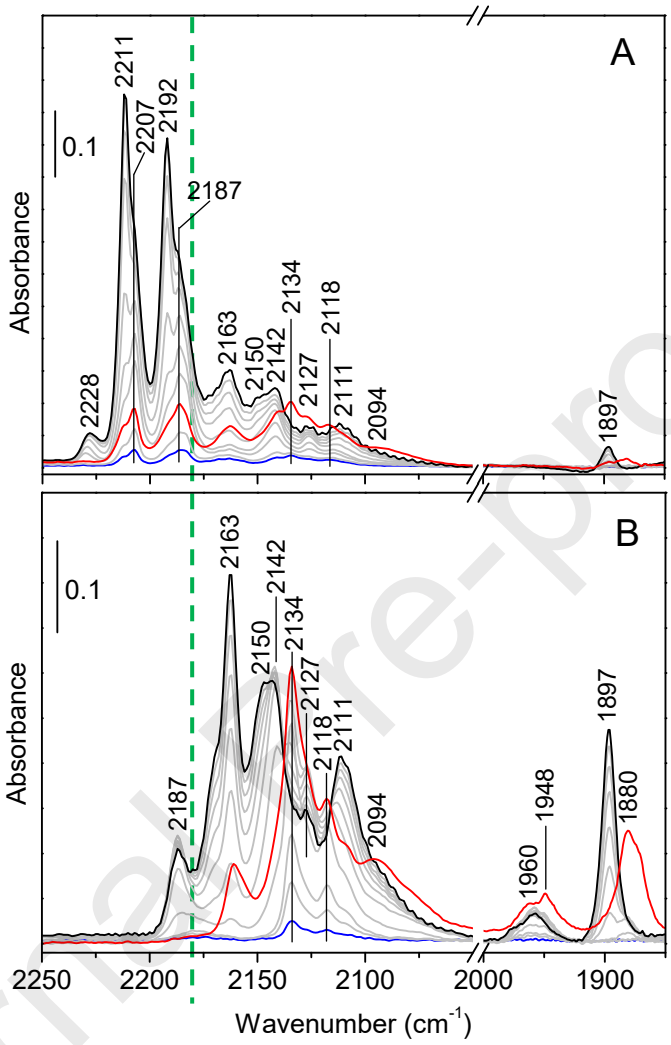

Fig. 4 FT-IR spectra of CO adsorbed at RT and at increasing pressure up to 20 mbar (from blue to black trace) on oxidized Pd(i)/SSZ-13 under dry conditions (A) and after pre-hydration (B). Red trace: spectrum run after CO outgassing at RT. Green dotted line: separation between high- and low-wavenumber bands.

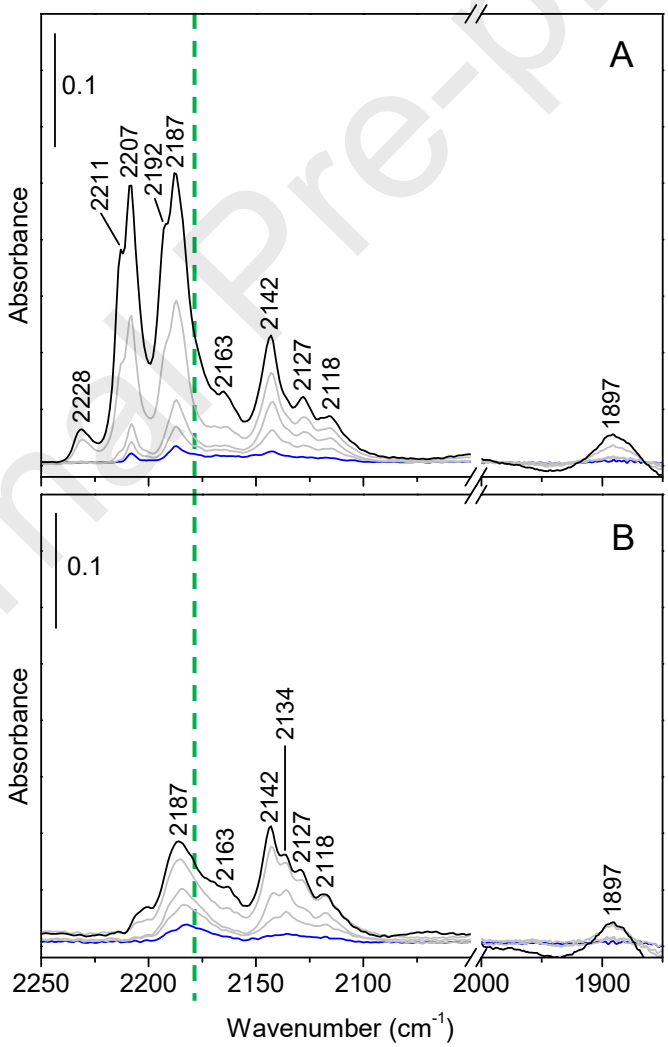

Fig. 5 FT-IR spectra of CO adsorbed at T_{LN} and at increasing pressure up to 0.1 mbar (from blue to black trace) on oxidized Pd(i)/SSZ-13 under dry conditions (A) and after pre-hydration at RT (B). Green dotted line: separation between high- and low-wavenumber bands.

The comparison of spectra collected for the anhydrous and pre-hydrated sample (Figure 5A and B, respectively) clearly shows that the low-wavenumber bands exhibit similar intensities in the two conditions. This result rules out the possibility that the bands in the low-wavenumber region are related to carbonyls of hydrated species of Pd^{2+} formed by pre-hydration at RT, since their intensities should be much more intense under wet conditions with respect to the dry ones, as in fact observed at RT (see Figure 3 and Figure 4). Accordingly, they should be related to Pd^{+} species present on the sample after calcination, since at T_{LN} any reduction of Pd^{2+} by CO can be excluded. These results hence indicate that the erosion of the high-wavenumber bands and the corresponding increase of the low-wavenumber ones observed at RT in Figure 3B are related to the reduction of Pd^{2+} sites by CO in the presence of water (reaction (1)), resulting in Pd^{+} formation. Notably, water is necessary in the reduction process not only for compensating with H^{+} the zeolite exchange sites set free by Pd reduction, but also for mobilizing Pd^{2+} cations and making possible reaction (1). Indeed, Mandal et al. reported the results of the mobility analysis for H_2O-solvated Pd complexes, which are detached from the zeolite framework.[21] They observed that the Pd mobility is enhanced as the degree of hydration is increased, finding that at the 2Al site the lowest free energy structure is $Z_2[Pd^{2+}(H_2O)_4]$ and at 1Al site is $Z[(PdOH)^{+}(H_2O)_3]$. Reaction (1) implies the involvement of two Pd^{2+} cations and the hydration

facilitates their interaction. By freezing at T_{LN}, also the movement of hydrated species is inhibited and this further confirms the hypothesis of CO reactivity promoted by water at RT.

It is worth of noting that at T_{LN} on pre-hydrated sample, no bands related to carbonyls of Pd^{2+} are formed in the high-wavenumber region (Figure 5B), except for that at 2187 cm^{-1}, even if no reduction of Pd^{2+} occurs. This could be ascribed to the stability of hydrated complexes of Pd^{2+}, such as $Z_2[Pd^{2+}(H_2O)_4]$ and $Z[(PdOH)^+(H_2O)_3]$, on which CO cannot be adsorbed: as a matter of facts, Mandal et al. calculated that these complexes are more stable than the corresponding complexes of isolated Pd^+.[21] Reasonably, the bond with H_2O is stronger than that with CO and this prevents CO being bonded to the $Z_2[Pd^{2+}(H_2O)_4]$ and $Z[(PdOH)^+(H_2O)_3]$ species. The same absence of bands related to carbonyls of Pd^{2+} in the high-wavenumber region, except for that at 2187 cm^{-1}, is observed at RT on the pre-hydrated sample (see Figure 4B): it is reasonable that at RT the mobility of the hydrated species guarantees the reduction by CO and the so formed Pd^+ ions bind CO stronger than H_2O. Therefore, at RT on the pre-hydrated sample upon increasing CO pressure, carbonyl species of Pd^{2+} are not detected, but those of Pd^+ are suddenly formed. We believe that Pd^+ species are not hydrated since the same bands are observed over the sample outgassed at 500 °C (see Figure 3A) for which the presence of hydrated Pd species is unlikely. Therefore, all the identified carbonyls are assigned to anhydrous Pd^+ species (see Table 1).

At this point, although the precise band assignments are not made yet, we can anyway conclude that the high-wavenumber bands are related to carbonyls of Pd^{2+} and the low-wavenumber ones are related to carbonyls of Pd^+ and Pd^0. It is worth of noting that Pd^+ species also exist in low amount even after oxidation at 500 °C (see Figures 3A, 5A and 5B).

To deepen the CO reactivity in the presence of water, it is necessary to take into account that, as reported by some authors, hydrated species $Z[PdOH]^+$, can also be involved in the reaction with CO as follows:[32,33]

$$CO + 2\ Z[PdOH]^+ \rightarrow CO_2 + 2\ ZPd^+ + H_2O \qquad (2)$$

In this case, $Z[PdOH]^+$ species is an intermediate formed by the following dissociative adsorption of water:

$$Z_2Pd^{2+} + H_2O \rightarrow Z[PdOH]^+ + ZH^+ \qquad (3)$$

Taking into account that Mandal et al. found that, in the presence of water, at the 2Al site the lowest free energy structure is $Z_2[Pd^{2+}(H_2O)_4]$ and at 1Al site is $Z[(PdOH)^+(H_2O)_3]$,[21] it is reasonable that also this hydrated species are involved in the reaction with CO. Thus, the water interested in the reaction can be adsorbed on the Brønsted sites of the zeolite (reaction(1)), as reported by Kim et al.,[25] or directly adsorbed on the exchanged Pd cations. To simplify the stoichiometry of the reactions, we can generally consider the involvement of adsorbed molecular water without specifying the adsorption site as follows:

$$CO + 2\ Z_2Pd^{2+} + H_2O \rightarrow CO_2 + 2\ ZPd^{+} + 2\ ZH^{+} \quad (4)$$

The sum of reaction (3) (multiplied by two) and reaction (2) gives reaction (4).

It is also possible to hypothesize a reduction process that leads up to the formation of metallic Pd as follows:

$$CO + Z_2Pd^{2+} + H_2O \rightarrow CO_2 + Pd^{0} + 2\ ZH^{+} \quad (5)$$

$$CO + 2ZPd^{+} + H_2O \rightarrow CO_2 + 2Pd^{0} + 2\ ZH^{+} \quad (6)$$

The occurrence of reactions (5) and (6) justifies the presence of the band at 1960 cm^{-1} (Figures 3B and 4B) assigned to bridged carbonyls of Pd^0 particles.[30,31]

3.4. Assignments of the Pd carbonyl bands

After determining that the high-wavenumber bands and the low-wavenumber ones are related to carbonyls of Pd^{2+} and Pd^{+} / Pd^0, respectively, the assignment of each band inside the two spectral regions has to be defined. This can be done on the basis of the effect of the operating conditions (contact time, P_{CO}, water presence, temperature) on the FT-IR spectra. In fact, as mentioned above, the evolution of the bands observed upon increasing CO pressure under dry and wet conditions points out specific behaviors that enable band assignments to Pd cations in different coordination. For this purpose, we have to go back to a deeper analysis of Figure 4; in particular, Figure 4A and 4B are suitable to examine the high- and the low-wavenumber bands, respectively. Band assignments discussed in the following are summarized in Table 1.

Due to the σ-donation character of the Pd^{2+}-CO bond, in the high-wavenumber region, i.e. 2220-2180 cm^{-1}, the higher the band frequency, the more coordinatively unsaturated the site.[30] In Figure 4A, at low CO pressure (blue trace) and after CO outgassing (red trace) the main bands in this region are at 2207 and 2187 cm^{-1}. The band at 2187 cm^{-1} is the only one belonging to the high-wavenumber region also present after water addition on the pre-adsorbed CO (Figure 3B) and on the pre-hydrated sample both during CO adsorption at RT and T_{LN} (Figure 4B and 5B). This means that the corresponding species: (i) is only slightly eroded by the reduction process operated by CO at RT in the presence of water and (ii) remains accessible to CO at T_{LN} differently from the other Pd^{2+} species. For these reasons, the band at 2187 cm^{-1} is assigned to CO adsorbed on Pd^{2+} sites belonging to PdO particles, whose presence is enlightened by TEM and HR-TEM images (see Figure 1). On the other hand, the band at 2207

cm^{-1} appears at low CO pressure (Figure 4A, blue trace), almost disappears on increasing CO coverage (Figure 4A, gray traces up to black trace) and eventually appears again after outgassing (Figure 4A, red trace). At the same time bands at 2211 and 2192 cm^{-1} increase upon increasing CO pressure and eventually disappear after outgassing. This behavior allows to recognize the presence of mono-carbonyls (band at 2207 cm^{-1}) that become di-carbonyls upon increasing CO pressure (bands at 2211 and 2192 cm^{-1}, $\nu_{asym}(CO)$ and $\nu_{sym}(CO)$ modes, respectively) and come back to mono-carbonyl species upon outgassing. Di-carbonyls are usually formed on sites characterized by low coordination number. Thus, these bands are likely related to mono- and di-carbonyls of isolated Pd^{2+} ions formed by ion exchange with the Brønsted acid sites and stabilized by the zeolite framework.[34,35]

Concerning the low-wavenumber region, i.e. below 2180 cm^{-1}, the bands are the same both under dry and wet conditions, but we use the spectra obtained on the pre-hydrated sample, since the higher band intensities allow to follow better the evolution with CO pressure (Figure 4B). Due to the π-backdonation contribution to the Pd^{+}-CO bond, the lower the band frequency, the more coordinatively unsaturated the site.[30] For this reason, the band at 2163 cm^{-1} is assigned to CO adsorbed on Pd^{+} sites belonging to Pd_2O particles. The increase of this band in the presence of CO and water at RT could be related to the reduction of Pd^{2+} sites belonging to particles. However, sites on particles do not need water to be reduced, according to the reaction:

$$CO + PdO \rightarrow CO_2 + Pd_2O \quad (7)$$

It is necessary to take into account that: (i) the band at 2163 cm^{-1} needs water to increase in intensity in the presence of CO; (ii) the increase in its intensity does not correspond to an erosion of similar intensity of the band at 2187 cm^{-1} related to carbonyls of Pd^{2+} on particles (see Figure 3B and 4B). For these reasons, it is reasonable that Pd^{+} sites on particles derive from the aggregation of some isolated Pd^{+} cations formed by the reduction of isolated Pd^{2+} sites and mobilized by hydration:[19]

$$2\ ZPd^{+} + H_2O \rightarrow Pd_2O + 2\ ZH^{+} \quad (8)$$

The significant increase of the band at 2163 cm^{-1} is also accompanied by a notable increase of the band at 1897 cm^{-1}; this latter band is attributed to bridged carbonyls of Pd^{+} belonging to Pd_2O particles [30] and the correlated behavior of both bands confirms these assignments. The band at 1897 cm^{-1} disappears after outgassing (red trace in Figure 4A) and a band at 1880 cm^{-1} appears. It is worth of noting that the band at 1880 cm^{-1} is already present at the beginning of the CO adsorption and disappears upon increasing CO pressure, while the band at 1897 cm^{-1} increases. The position and the behavior of the band at 1880 cm^{-1} upon CO pressure change and subsequent outgassing suggest the assignment to multi-bridged carbonyls of Pd^{+} belonging to particles, i.e. $Pd_n^{+}(CO)$ with n >2.

As evidenced in the high-wavenumber region, also in the low-wavenumber one, the behavior of some bands upon changing the CO coverage allows to recognize the presence of mono-carbonyls that become di-carbonyls. This is the case of bands at 2134 and 2118 cm^{-1} that appear

at very low CO pressure (Figure 4B, blue trace), disappear on increasing pressure (Figure 4B, gray traces up to black trace) and then appear again after outgassing (Figure 4B, red trace). At the same time, upon increasing CO pressure, bands at 2150, 2142, 2127 and 2111 cm^{-1} increase and are eroded during the outgassing. Therefore, it is possible to recognize the presence of two mono-carbonyl species (bands at 2134 and 2118 cm^{-1}) that evolve in four bands related to di-carbonyls (bands at 2150, 2142, 2127 and 2111 cm^{-1}). As mentioned above, di-carbonyls are usually formed on sites characterized by low coordination number. This implies the presence of two different isolated Pd^{+} species at the exchange sites of the zeolite: indeed, Pd^{+} can be located into 8 member-rings and 6-member rings of the zeolite framework.[18,21,30] In the measurement performed at constant CO pressure (20 mbar), the formation of Pd^{+} di-carbonyls occurs directly (as shown in Figure 3) without going through the mono-carbonyl species, due to the high CO pressure. In particular, the data shown in Figure 3B allow to correlate the bands due to the same di-carbonyls: in the spectra, bands at 2150 and 2111 cm^{-1} are markedly more intense than those at 2142 and 2127 cm^{-1}. Therefore, we assign the couple of bands at 2150 and 2111 cm^{-1} to one of the di-carbonyl species and the couple at 2142 and 2127 cm^{-1} to the other di-carbonyl species. Moreover, the spectra obtained at T_{LN} (Figure 5) allow to correlate the two couples of di-carbonyl bands to the corresponding mono-carbonyl band. Indeed, on one hand the band of mono-carbonyl at 2118 cm^{-1} is not eroded upon increasing CO coverage and the di-carbonyl bands at 2150 and 2111 cm^{-1} are not formed; on the other hand, the mono-carbonyl band at 2134 cm^{-1} is very weak and the di-carbonyl bands at 2142 and 2127 cm^{-1} are well visible. Thus, the mono-carbonyl band at 2118 cm^{-1} is correlated to the di-carbonyl bands at 2150 and 2111 cm^{-1} and the mono-carbonyl band at 2134 cm^{-1} is correlated to the di-carbonyl bands at 2142 and 2127 cm^{-1}, as reported in Table 1.

Outside the spectral regions of Pd carbonyls, the weak band at 2228 cm^{-1} can be assigned to CO bonded to extra-framework Al^{3+}.[36] This band is present only under dry conditions (see Figures 3, 4 and 5), reasonably due to the steric hindrance of adsorbed molecular water under wet conditions. Finally, a broad absorption at 2094 cm^{-1} appears after CO outgassing both under dry and wet conditions (Figure 4A and 4B, red trace) and, referencing to literature data, it is a typical position of Pd^{0}(111) linear carbonyls.[30,31] This band is particularly evident after outgassing under wet conditions, when another band at 1948 cm^{-1} is evident after outgassing: the latter is characteristic of bridged CO on Pd^{0}(111), being at 2094 cm^{-1} the correspondent band related to linear carbonyls of Pd^{0}(111).[31] Reasonably, some oxygen species on PdO_x particles are removed along with CO during the outgassing, changing oxidized Pd^{n+} sites on PdO_x particle surface into Pd^{0} sites. Since PdO_x particles, in particular Pd_2O, are more abundant under wet conditions, Pd^{0}(111) sites are formed in larger amount under wet conditions, but their formation is also observed on anhydrous sample, demonstrating that in this process water is not necessary. As already reported above, another band at 1960 cm^{-1} related to bridged carbonyls of Pd^{0}(100) is observed in the presence of both CO and water and is already visible before outgassing (see Figures 3B and 4B). These last Pd^{0} sites need water to form and the occurrence of reactions (5) and (6) has been hypothesized as reported above. Therefore, on one hand Pd^{0}(100) sites are formed by aggregation and reduction of isolated Pd^{2+} / Pd^{+} cations in the presence of CO and water, on the other hand Pd^{0}(111) sites are originated during CO outgassing, with and without water, by the reduction of Pd^{2+} / Pd^{+} sites at the surface of PdO_x particles.

The discussion reported above is based on experiments obtained in the case of the impregnated sample (Pd(i)/SSZ-13). In Figure 6, the spectra of the ion exchanged sample obtained at increasing CO pressure under dry conditions (panel A) and after pre-hydration (panel B) are shown. By the comparison with Figure 4, which shows the results of the experiments carried out under the same conditions with the impregnated sample, it is well

evident the presence of the same bands with the same behaviors for the two samples. The lower band intensities in Figure 6 are related to the lower Pd loading for Pd(ie)/SSZ-13 with respect to Pd(i)/SSZ-13 (0.2 vs. 1 wt.%). This clearly indicates that the behavior of the sample prepared by ion-exchange is overlapped with that of the impregnated one discussed above.

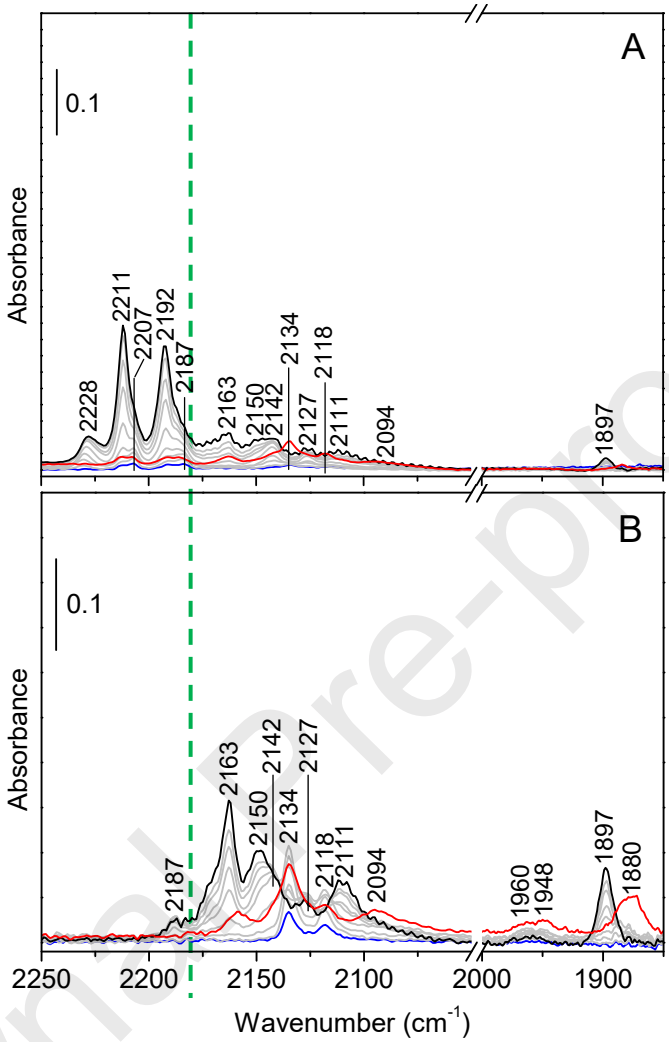

Fig. 6 FT-IR spectra of CO adsorbed at RT and at increasing pressure up to 20 mbar (from blue to black trace) on oxidized Pd(ie)/SSZ-13 under dry conditions (A) and after pre-hydration (B). Red trace: spectrum run after CO outgassing at RT. Green dotted line: separation between high- and low-wavenumber bands.

Tab. 1 Carbonyl species assignments.

Species	Pd coordination	ν (cm^{-1})
Al^{3+}(CO)	-	2228
$Pd^{2+}(CO)_2$	isolated at the exchange sites of the zeolite	2211 (asym.), 2192 (sym.)
Pd^{2+}(CO)	isolated at the exchange sites of the zeolite	2207
Pd^{2+}(CO)	PdO particles	2187
Pd^{+}(CO)	Pd_2O particles	2163
Pd_2^{+}(CO)	Pd_2O particles	1897
Pd_n^{+}(CO), n >2	Pd_2O particles	1880
$Pd^{+}(CO)_2$ (species 1)	isolated at the exchange sites of the zeolite	2150 (asym.), 2111 (sym.)

$Pd^{+}(CO)$ (species 1)	isolated at the exchange sites of the zeolite	2118
$Pd^{+}(CO)_2$ (species 2)	isolated at the exchange sites of the zeolite	2142 (asym.), 2127 (sym.)
$Pd^{+}(CO)$ (species 2)	isolated at the exchange sites of the zeolite	2134
$Pd^{0}(CO)$	$Pd^{0}(111)$	2094
$Pd_2^{0}(CO)$	$Pd^{0}(111)$	1948
$Pd_2^{0}(CO)$	$Pd^{0}(100)$	1960

4. Conclusions

The present work reports the results of a study on Pd speciation in Pd/SSZ-13 samples prepared by different methods, i.e. impregnation and ion exchange. The characterization was performed by FT-IR spectroscopy of CO adsorbed at different temperatures (RT and liquid nitrogen temperature, T_{LN}), P_{CO}, contact time and on anhydrous and hydrated sample. This allowed a clear identification and characterization of the Pd sites in terms of oxidation states and coordination degrees, and the rationalization of the effect of water on the Pd reduction by CO.

In particular, we showed that, in the case of the impregnated Pd/SSZ-13 sample, carbonyl bands in the spectral region 2220-2180 cm^{-1} are mainly related to isolated Pd^{2+} cations at the exchange sites of the zeolite. By the combined effect of CO and adsorbed water at RT, these sites are reduced to isolated Pd^{+} sites, whose carbonyl bands fall in the spectral region 2150-2100 cm^{-1}. The aggregation of some Pd^{+} sites, just formed by the reduction and mobilized by the hydration, gives rise to the formation of Pd_2O particles. Also, CO adsorption under dry and wet conditions highlights the presence of PdO particles, which are already present on the external surface of the zeolite in the oxidized sample prior to the mobility effect induced by water; this observation is consistent with the findings from TEM and HR-TEM images. The presence of CO and water does not significantly alter these PdO particles. At wavenumbers lower than 2100 cm^{-1}, band related to bridged carbonyls of $Pd^{0}(100)$ sites is observed with CO

on hydrated sample, evidencing a strong reducing effect of CO on isolated Pd^{2+} / Pd^{+} ions in the presence of water at RT. Pd^0 sites are formed by the aggregation and reduction of isolated Pd cations. Other Pd^0 sites are formed during CO outgassing both under dry and wet conditions: these are Pd^0(111) sites formed on the surface of PdO_x particles during the CO outgassing. In this last process, water is not involved.

The key measurements for understanding the reducing effect of CO in the presence of water were performed at liquid nitrogen temperature: the quenching of any reactivity at very low temperature allowed us to exclude the presence of carbonyls related to hydrated Pd^{2+} species. The low temperature measurements make also apparent the role of the Pd cation mobility in the reduction process: indeed, the reduction process implies the involvement of a couple of Pd cations and hydration facilitates their interaction. By freezing at T_{LN}, also the movement of hydrated species is inhibited and this further confirms the hypothesis that water promotes CO reactivity at RT. Accordingly water is necessary not only for compensating with H^+ the zeolite exchange sites set free by Pd reduction, but also for mobilizing isolated Pd^{2+} / Pd^{+} cations and making possible the reduction reactions. Moreover, the Pd ion mobility promoted by water makes the formation of Pd_2O particles and Pd^0 sites possible.

The hydration of the sample was performed both after and before CO adsorption: in both cases, Pd reduction is obtained. On the pre-hydrated sample, at low temperature the hindering of Pd^{2+} cations by adsorbed water towards CO is put in evidence. This is related to the stability of the complexes that isolated Pd^{2+} formed with water, more stable than those of isolated Pd^{+}. Moreover, pre-adsorbed water avoids the CO bond with isolated Pd^{2+} cations, but not the Pd^{2+} reduction into Pd^{+} and Pd^0, which, once formed, are able to coordinate CO.

Finally, it was found that the impregnated and ion exchanged samples gave the same spectroscopic results in terms of band positions and behaviors. However, they showed different carbonyl band intensities, as expected in view of the different Pd content (0.2 and 1 wt.% for the ion exchanged and impregnated sample, respectively).

Author Contributions

S. Morandi: Conceptualization, Investigation, Methodology, Writing – original Draft. **L. Castoldi:** Writing – review & editing, Methodology. **R. Matarrese:** Writing – review & editing, Methodology. **L. Lietti:** Supervision, Writing – review & editing.

Conflicts of interest

There are no conflicts to declare.

Acknowledgements

S. Morandi acknowledges the support from Project CH4.0 under the MUR (Italian Ministry for the University) program “Dipartimenti di Eccellenza 2023–2027” (CUP: D13C22003520001).

References

1 P. Bayer and C. Schüth, *Water Sci. & Tech.*, 2010, **62**, 708.

2 H. Azzi, K. Bendahou, L. Cherif-Aouali, F. Hamidi, S. Siffert, A. Bengueddach and A. Aboukais, *Chem. Today*, 2012, **30**, 28.

3 M. Mora, C. Jiménez-Sanchidrián and J. R. Ruiz, *Current Org. Chem.*, 2012, **16**, 1128.

4 S. Sadjadi and M. M. Heravi, *RSC Adv.*, 2016, **6**, 88588.

5 A. Kumbhar, *Top. Current Chem.*, 2017, **375**.

6 X. Zhang, X. Chen, Y. Liu and M. Guo, *Water, Air, and Soil Pollut.*, 2020, **231**.

7 H. W. Zhao, A. J. Hill, L. Ma, A. Bhat, G. H. Jing and J. W. Schwank, *Catal. Sci. & Tech.*, 2021, **11**, 5986.

8 H. Y. Chen, J. Lu, J. M. Fedeyko and A. Raj, *Appl. Catal. A: Gen.*, 2022, **633**.

9 H. Cheng, X. Tang, H. Yi, R. Pan, J. Zhang, F. Gao and Q. Yu, *Chem. Eng. J.*, 2022, **449**.

10 Á. Mastalir and Á. Molnár, *Coord. Chem. Rev.*, 2022, **470**.

11 W. S. Epling, L. E. Campbell, A. Yezerets, N. W. Currier and J. E. Parks, *Catal. Rev.-Sci. and Eng.*, 2004, **46**, 163.

12 A. M. Beale, F. Gao, I. Lezcano-Gonzalez, C. H. F. Peden and J. Szanyi, *Chem. Soc. Rev.*, 2015, **44**, 7371.

13 C. K. Lambert, *Reac. Chem. & Eng.*, 2019, **4**, 969.

14 J. R. Theis and C. K. Lambert, *Catal. Today*, 2015, **258**, 367.

15 Y. T. Gu and W. S. Epling, *Appl. Catal. A-Gen.*, 2019, **570**, 1.

16 J. Lee, J. R. Theis and E. A. Kyriakidou, *Appl. Catal. B-Env.*, 2019, **243**, 397.

17 Y. Zheng, L. Kovarik, M. H. Engelhard, Y. L. Wang, Y. Wang, F. Gao and J. Szanyi, *J. Phys. Chem. C*, 2017, **121**, 15793.

18 R. B. Pace, T. M. Lardinois, Y. Y. Ji, R. Gounder, O. Heintz and M. Crocker, *ACS Omega*, 2021, **6**, 29471.

19 T. M. Lardinois, K. Mandal, V. Yadav, A. Wijerathne, B. K. Bolton, H. Lippie, C. W. Li, C. Paolucci and R. Gounder, *J. Phys. Chem. C*, 2022, **126**, 8337.

20 R. Matarrese, L. Castoldi, S. Morandi, P. Ticali, M. C. Valsania and L. Lietti, *Appl. Catal. B-Env.*, 2023, **331**, 15.

21 K. Mandal, Y. T. Gu, K. S. Westendorff, S. C. Li, J. A. Pihl, L. C. Grabow, W. S. Epling and C. Paolucci, *ACS Catal.*, 2020, **10**, 12801.

22 C. Paolucci, A. A. Parekh, I. Khurana, J. R. Di Iorio, H. Li, J. D. A. Caballero, A. J. Shih, T. Anggara, W. N. Delgass, J. T. Miller, F. H. Ribeiro, R. Gounder and W. F. Schneider, *J. Am. Chem. Soc.*, 2016, **138**, 6028.

23 I. Song, K. Khivantsev, Y. Wang and J. Szanyi, *J. Phys. Chem. C*, 2022, **126**, 1439.

24 I. Song, K. Khivantsev, Y. Q. Wu, M. Bowden, Y. Wang and J. Szanyi, *Appl. Catal. B-Env.*, 2022, **318**.

25 P. Kim, J. van der Mynsbrugge, M. Head-Gordon and A. T. Bell, *J. Phys. Chem. C*, 2022, **126**, 18744.

26 L. Castoldi, S. Morandi, P. Ticali, R. Matarrese and L. Lietti, *Catalysts*, 2023, **13**, 14.

27 M. Krossner and J. Sauer, *J. Phys. Chem.*, 1996, **100**, 6199.

28 F. Wakabayashi, J. N. Kondo, K. Domen and C. Hirose, *J. Phys. Chem.*, 1996, **100**, 1442.

29 A. Zecchina, S. Bordiga, G. Spoto, D. Scarano, G. Petrini, G. Leofanti, M. Padovan and C. O. Arean, *J. Chem. Soc.-Faraday Trans.*, 1992, **88**, 2959.

30 K. I. Hadjiivanov and G. N. Vayssilov, in *Adv. Catal.*, eds. B. C. Gates and H. Knozinger, 2002, vol. 47, pp. 307.

31 E. Groppo, S. Bertarione, F. Rotunno, G. Agostini, D. Scarano, R. Pellegrini, G. Leofanti, A. Zecchina and C. Lamberti, *J. Phys. Chem. C*, 2007, **111**, 7021.

32 M. Ambast, A. Gupta, B. M. M. Rahman, L. C. Grabow and M. P. Harold, *Appl. Catal. B-Env.*, 2021, **286**.

33 R. Villamaina, U. Iacobone, I. Nova, E. Tronconi, M. P. Ruggeri, L. Mantarosie, J. Collier and D. Thompsett, *Appl. Catal. B-Env.*, 2021, **284**.

34 K. Khivantsev, F. Gao, L. Kovarik, Y. Wang and J. Szanyi, *J. Phys. Chem. C*, 2018, **122**, 10820.

35 K. Khivantsev, N. R. Jaegers, I. Z. Koleva, H. A. Aleksandrov, L. Kovarik, M. Engelhard, F. Gao, Y. Wang, G. N. Vayssilov and J. Szanyi, *J. Phys. Chem. C*, 2020, **124**, 309.

36 B. Onida, F. Geobaldo, F. Testa, F. Crea and E. Garrone, *Micropor. Mesopor. Mat.*, 1999, **30**, 119.

Graphical Abstract

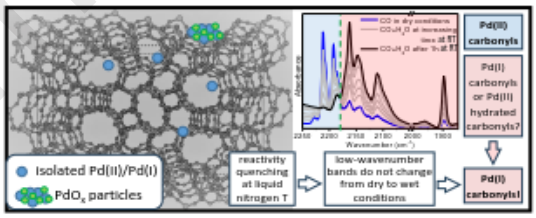

Highlights

- FTIR spectroscopy of adsorbed CO on impregnated and ion exchanged Pd/SSZ-13 samples
- CO reducing effect on Pd^{2+} only in the presence of H_2O
- H_2O compensates with H^+ the zeolite exchange sites set free by Pd reduction
- H_2O mobilizes isolated Pd cations, making possible the reduction reactions
- Combined effect of H_2O and CO allow to detail the assignments of carbonyl IR bands

Declaration of interests

☒ The authors declare that they have no known competing financial interests or personal relationships that could have appeared to influence the work reported in this paper.

☐ The authors declare the following financial interests/personal relationships which may be considered as potential competing interests: